Hindawi Publishing Corporation
Research Letters in Signal Processing
Volume 2008, Article ID 932068, 5 pages
doi:10.1155/2008/932068

Research Letter

An Adaptive Resolution Computationally Efficient Short-Time Fourier Transform

Saeed Mian Qaisar, Laurent Fesquet, and Marc Renaudin

TIMA, CNRS UMR 5159, 46 avenue Felix-Viallet, 38031 Grenoble Cedex, France

Correspondence should be addressed to Saeed Mian Qaisar, saeed.mian-qaisar@imag.fr

Received 31 January 2008; Accepted 22 April 2008

Recommended by Sos Agaian

The short-time Fourier transform (STFT) is a classical tool, used for characterizing the time varying signals. The limitation of the STFT is its fixed time-frequency resolution. Thus, an enhanced version of the STFT, which is based on the cross-level sampling, is devised. It can adapt the sampling frequency and the window function length by following the input signal local characteristics. Therefore, it provides an adaptive resolution time-frequency representation of the input signal. The computational complexity of the proposed STFT is deduced and compared to the classical one. The results show a significant gain of the computational efficiency and hence of the processing power.

1. INTRODUCTION

Most of the real-life signals like speech, Doppler, seismic, and biomedical signals are time varying in nature. The spectral contents of these signals vary with time, which is a direct consequence of the signal generation process [1]. The STFT is a classical tool for characterizing such signals [2]. The limitation with the STFT is that it provides a fixed resolution time-frequency representation of the input signal. This fixed resolution is the reason for the creation of the multiresolution analysis (MRA) techniques [3–5], which provide a good frequency but a poor time resolution for the low-frequency events and a good time but apoor frequency resolution for the high-frequency events. This type of analysis is well suited for most of the real-life signals [3].

In this article, the fixed resolution dilemma is resolved to a certain extent by revising the STFT. The motivation behind the proposed STFT is to achieve a smart time-frequency representation of the time varying signals. The idea is to adapt the time-frequency resolution along with the computational load by following the input signal local characteristics. An efficient solution is proposed by smartly combining the features of both uniform and nonuniform signal processing tools.

2. PROPOSED ADAPTIVE RESOLUTION STFT

The block diagram of the proposed STFT is shown in Figure 1. The description of different blocks is given below.

2.1. Asynchronous analog to digital converter (AADC)

According to [6], the sampling instants of a nonuniformly sampled signal obtained with the level crossing sampling scheme (LCSS) are defined by (1). Where t_n is the current sampling instant, t_{n-1} is the previous one, and dt_n is the time delay between the current and the previous sampling instants (cf. (2)).

The LCSS drastically reduces the activity of the post processing chain, because it only captures the relevant information [7–9]. In this context, analog to digital converters based on the LCSS have been developed [10–12]. The AADC [10] is employed for digitizing $x(t)$. An *M-bit* resolution AADC has $2^M - 1$ quantization levels which are uniformly disposed according to $x(t)$ amplitude dynamics. The AADC has a finite bandwidth. Thus, to assure a proper signal capturing a band pass filter with pass band $[f_{\min}; f_{\max}]$ is employedat the AADC input. Let ΔV_{in} and $\Delta x(t)$ be the AADC and $x(t)$ amplitude dynamics, respectively. In order to avail the complete AADC resolution in the studied case,

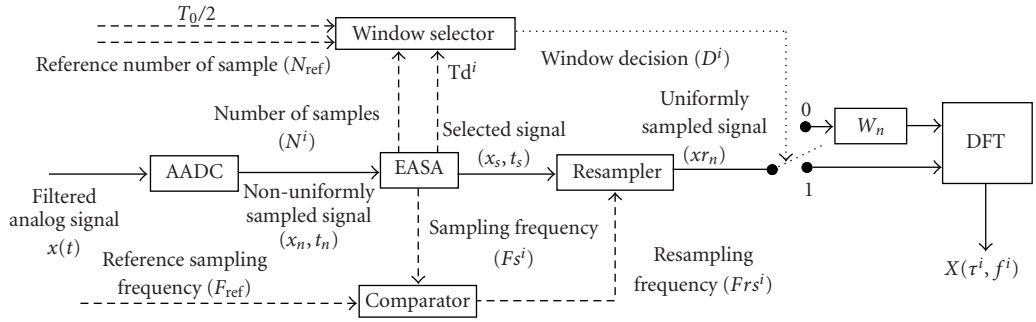

Figure 1: Block diagram of the proposed STFT. "—" represents the signal flow, "....." represents the control flow, and "- - - - -" represents the parameters flow, at system different stages.

While ($dt_n \le T_0/2$ and $N^i \le N_{ref}$)
$N^i = N^i + 1$;
end

Algorithm 1: Enhanced activity selection algorithm (EASA).

$\Delta x(t)$ is always adapted to match ΔV_{in}. For an AADC, the maximum and the minimum sampling frequencies [7] are defined by (3) and (4), respectively. Where, Fs_{max} and Fs_{min} are the maximum and the minimum sampling frequencies of the AADC. f_{max} is the bandwidth and f_{min} is the fundamental frequency of $x(t)$:

$$t_n = t_{n-1} + dt_n, \tag{1}$$

$$dt_n = t_n - t_{n-1}, \tag{2}$$

$$Fs_{max} = 2 \cdot f_{max} \cdot (2^M - 1), \tag{3}$$

$$Fs_{min} = 2 \cdot f_{min} \cdot (2^M - 1). \tag{4}$$

2.2. Enhanced activity selection algorithm (EASA) and window selector

The relevant parts of the nonuniformly sampled signal obtained with the AADC are selected—corresponds to the variable length rectangular window—by the EASA. The EASA is defined as shown in Algorithm 1. $T_0 = 1/f_{min}$ is the fundamental period of $x(t)$. T_0 and dt_n detect parts of the nonuniformly sampled signal with activity. The condition on dt_n is chosen in order to satisfy the Nyquist criterion for f_{min}, when sampling $x(t)$ nonuniformly with the AADC [13]. N^i represents the number of nonuniform samples lie in the ith selected window, which lie on the jth active part of the nonuniformly sampled signal. Where, i and j both belong to the set of natural numbers $\mathbb{N}^*$. N_{ref} represents the upper bound on N^i. The choice of N_{ref} depends on $x(t)$ characteristics and on system parameters. The above described loop repeats for each selected window, which occurs during the observation length of $x(t)$. Every time before repeating the loop, i is incremented and N^i is initialized to zero.

The EASA displays interesting features with the LCSS, which are not available in the classical case. It selects only the active parts of the nonuniformly sampled signal, obtained with the AADC. Moreover, it correlates the length of the selected window with the signal local characteristics.

The window selector implements the condition given by expression (5). Jointly, the EASA and the window selector provide an efficient spectral leakage reduction in the case of transient signals [13]. Indeed, spectral leakage occurs due to the signal truncation problem. Usually an appropriate smoothening (cosine) window function is employed to reduce the signal truncation. For the proposed case, as long as the condition 5 is true, the leakage problem is resolved by avoiding the signal truncation. As no signal truncation occurs so no cosine window is required. In this case the window decision $D^i = 1$, which makes the switch state 1 (cf. (Figure 1)). Otherwise, an appropriate cosine window is employed to reduce the signal truncation problem. In this case $D^i = 0$, which makes the switch state 0. In expression 5, t_1^i represents the 1st sampling instant of the ith selected window and t_{end}^{i-1} represents the last sampling instant of the $(i-1)$th selected window.

For proper spectral representation, the condition given by expression (6) should be satisfied [13]. Where, L^i is the length in seconds of the ith selected window. In order to satisfy this condition for the worst case, which occurs for Fs_{max}, N_{ref} is calculated for an appropriate reference window length L_{ref}. Where, L_{ref} satisfies the condition $L_{ref} \ge T_0$. The process is given by (7) as follows:

$$\text{if } \left(N^i \le N_{ref} \text{ and } (Td^i = t_1^i - t_{end}^{i-1}) > \frac{T_0}{2}\right), \tag{5}$$

$$L^i \ge T_0, \tag{6}$$

$$N_{ref} = L_{ref} \cdot Fs_{max}. \tag{7}$$

The lower and the upper bounds on L_{ref} are posed, respectively, by T_0 and the system resources (the maximum sample frame which the system can process at once). For N_{ref} (cf. (7)), the condition 6 holds for all selected windows except for the case when the actual length of the jth activity is less than T_0.

2.3. Adaptive sampling rate

The AADC sampling frequency is correlated to $x(t)$ local variations [7, 13]. Let Fs^i represent the AADC sampling frequency for the ith selected window. Fs^i can be calculated

by using (8). Where, $t\max^i$ and $t\min^i$ are the final and the initial times of the ith selected window. The upper and the lower bounds on Fs^i are posed by $Fs_{\max}$ and $Fs_{\min}$, respectively:

$$L^i = t\max^i - t\min^i.$$
$$Fs^i = \frac{N^i}{L^i}. \tag{8}$$

The selected data obtained with the EASA can be used directly for further nonuniform digital processing [8, 14]. However in the studied case, the selected data is resampled uniformly. It enables to take advantage of both nonuniform and uniform signal processing tools [7, 13]. Due to this resampling there will be an additional error. Nevertheless, prior to this transformation, one can take advantage of the inherent oversampling of the relevant signal parts in the system [7]. Hence, it adds to the accuracy of the post resampling process [11]. The nearest neighbour resampling interpolation (NNRI) is employed for data resampling. The reasons of inclination towards NNRI are discussed in [13, 15].

A reference sampling frequency F_{ref} is chosen, such as itremains greater than and closest to the $F_{\text{Nyq}} = 2\cdot f_{\max}$. Depending upon the values of F_{ref} and Fs^i, the resampling frequency Frs^i (cf. (Figure 1)) can be adapted for the ith selected window. For the case, $Fs^i > F_{\text{ref}}$, Frs^i is chosen as: $Frs^i = F_{\text{ref}}$. It is done in order to resample the selected data, lie in the ith selected window closer to the Nyquist frequency. It avoids the unnecessary interpolations during the data resampling process and so reduces the computational load of the proposed technique.

For the case, $Fs^i \le F_{\text{ref}}$, Frs^i is chosen as: $Frs^i = Fs^i$. In this case, it appears that the data lie in the ith selected window may be resampled at a frequency which is less than F_{Nyq} and so it can cause aliasing. Since, the sampling rate of the AADC varies according to the slope of $x(t)$ [10]. A high-frequency signal part has a high slope and the AADC samples it at a higher rate and vice versa. Hence, a signal part with only low-frequency components can be sampled by the AADC at a subNyquist frequency of $x(t)$. But still this signal part is locally oversampled in time with respect to its local bandwidth [7]. Hence, there is no danger of aliasing. This statement is further illustrated with the results summarized in Table 1.

2.4. Adaptive resolution analysis

The STFT of a sampled signal x_n is determined by computing the discrete Fourier transform (DFT) of an N samples segment centred on τ, which describes the spectral contents of x_n around the instant τ. Where N is defined as: $N = L\cdot Fs$. Here, L is the effective length in seconds of the window function w_n and Fs is the sampling frequency. The STFT can be expressed mathematically by (9). In Equation (9), f is the frequency index, which is normalized with respect to Fs.

L controls the STFT time and frequency resolution [2]. In the classical case, the input signal is sampled at a fixed sampling frequency Fs, regardless of its local variations. Thus, a fixed L results into a fixed N. In this case, the time resolution Δt and the frequency resolution Δf of the STFT can be defined by (10) and (11), respectively. Equation (11) shows that for a fixed Fs, Δf can be increased by increasing N. But increasing N requires to increase L which will reduce Δt (cf. (10)). Thus, a larger L provides a better Δf but a poor Δt, and vice versa. This conflict between Δf and Δt is the reason for the creation of the MRA techniques [3–5].

The proposed STFT is a smart alternative of the MRA techniques. It performs adaptive time-frequency resolution analysis, which is not attainable with the classical STFT. It is achieved by adapting the Frs^i, L^i, and Nr^i according to the local variations of $x(t)$. Nr^i is the number of resampled data points that lie in the ith selected window. Thus, the time resolution Δt^i and the frequency resolution Δf^i of the proposed STFT can be specific for the ith selected window and are defined by (12) and (13), respectively. Because of this adaptive resolution, the proposed STFT will be named as the adaptive resolution STFT, (ARSTFT) throughout the following parts of this article. The adaptation of Frs^i, L^i, and Nr^i also adds to the computational gain of the ARSTFT, compared to the classical one. It is achieved firstly by avoiding the unnecessary samples to process and secondly by avoiding the use of the cosine window function as far as the condition 5 is true. The ARSTFT is defined by (14). In (14), τ^i and f^i are the central time and the frequency index of the ith selected window, respectively. f^i is normalized with respect to Frs^i. n is the index of the resampled data points lie in the ith selected window. The notation w_n^i represents that the window function length L^i and shape (rectangle or cosine) can be adapted for the ith selected window:

$$X[\tau,\, f] = \sum_{n=\tau-L/2}^{\tau+L/2} [x_n\cdot w_{n-\tau}]\cdot e^{-j\cdot 2\pi\cdot f\cdot n}. \tag{9}$$

$$\Delta t = L. \tag{10}$$

$$\Delta f = \frac{Fs}{N}. \tag{11}$$

$$\Delta t^i = L^i. \tag{12}$$

$$\Delta f^i = \frac{Frs^i}{Nr^i}. \tag{13}$$

$$X[\tau^i,\, f^i] = \sum_{n=\tau^i-Nr^i/2}^{\tau^i+Nr^i/2} [\{\text{Re sample}(x_n,\, t_n)\}\cdot w_{n-\tau^i}^i]\cdot e^{-j\cdot 2\pi\cdot f^i\cdot n}. \tag{14}$$

3. ILLUSTRATIVE EXAMPLE

In order to illustrate the ARSTFT an input signal $x(t)$, shown on the left part of Figure 2 is employed. Its total duration is 30 seconds and it consists of three active parts. Each activity is a sinusoid of 0.9 v amplitude and of 50, 200, and 500 Hz frequency, respectively. The time length of each activity is 5, 0.5, and 1.6 seconds, respectively. $x(t)$ is band limited between 50 to 500 Hz and it is sampled by employing a 3-bit resolution AADC. Thus, $Fs_{\max}$ and $Fs_{\min}$ become 7 kHz and 0.7 kHz, respectively (3), (4). $F_{\text{ref}} = 1.25$ kHz and $\Delta V_{\text{in}} = 1.8$ v are chosen. The selected data obtained with the EASA is shown on the right part of Figure 2. By following the criteria

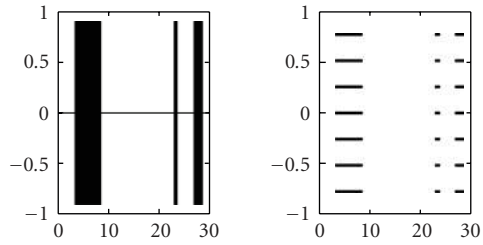

Figure 2: Input signal (left) and selected signal (right).

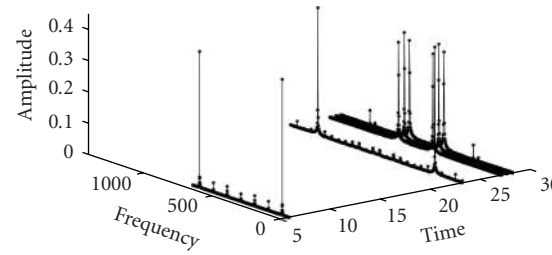

Figure 3: The ARSTFT of the selected windows.

Table 1: Summary of parameters of the selected windows.

Selected window	L^i (Sec)	Fs^i (kHz)	N^i (Smp)	F_{ref} (kHz)	Frs^i (kHz)	Nr^i (Smp)
1st	4.99	0.7	3500	1.25	0.7	3500
2nd	0.49	2.8	1400	1.25	1.25	625
3rd	0.58	7.0	4096	1.25	1.25	731
4th	0.58	7.0	4096	1.25	1.25	731
5th	0.43	7.0	3005	1.25	1.25	536

Table 2: Time and frequency resolution of the selected windows.

Window	1st	2nd	3rd	4th	5th
Δt^i(Sec)	4.99	0.49	0.58	0.58	0.43
Δf^i(Hz)	0.2	2.0	1.71	1.71	2.33

given in Section 2, $N_{\text{ref}} = 4096$ is chosen, which leads to 5 selected windows. First, two selected windows correspond to the first two activities and the remaining corresponds to the third activity. The last three selected windows are not distinguishable on the right part of Figure 2, because they lie consecutively on the third activity. The parameters of each selected window are summarized in Table 1.

Table 1 exhibits the interesting features of the ARSTFT. Fs^i represents the sampling frequency adaptation by following the local variations of $x(t)$. It is achieved due to the smart features of the AADC and the EASA. N^i shows that the relevant signal parts are locally oversampled in time with respect to their local bandwidths [7]. Frs^i shows the adaptation of the resampling frequency for each selected window. It further adds to the computational gain of the ARSTFT, by avoiding the unnecessary interpolations during the resampling process. Nr^i shows how the adaptation of Frs^i avoids the processing of unnecessary samples during the spectral computation. L^i exhibits the EASA dynamic feature, which is to correlate the window function length with the local variations of $x(t)$. Adaptation of L^i, Frs^i and Nr^i leads to the adaptive time-frequency resolution, which is clear from the values of Δt^i and Δf^i in Table 2.

Table 2 demonstrates that ARSTFT adapts its time-frequency resolution by following the local variations of $x(t)$. It provides a good time but a poor frequency resolution for the high frequency parts of $x(t)$, and vice versa. It is the type of analysis, well suited for most of the real-life signals [3]. The spectrum of each selected window is computed and plotted with respect to τ_i on Figure 3. Figure 3 shows the fundamental and the periodic spectrum peaks of each selected window. In this case, the spectrum periodic frequency for the ith selected window f_p^i is equal to Frs^i. It shows the adaptation of Frs^i, which can be visualized from Figure 3.

The ARSTFT also adapts the window shape (rectangle or cosine) for the ith selected window. The condition 5 remains true for the first two selected windows, which sets $D^i = 1$. As no signal truncation occurs so no cosine window is required in this case. On the other hand, the number of samples for the fourth activity is 11200. Therefore, $N_{\text{ref}} = 4096$ leads to the three selected windows for the time span of the fourth activity. The condition 5 becomes false in this case, which sets $D^i = 0$. As signal truncation occurs so suitable length cosine (Hanning) windows are employed to reduce this effect.

In the classical case, if $Fs = F_{\text{ref}}$ is chosen, in order to satisfy the Nyquist sampling criterion for $x(t)$. Then the whole signal will be sampled at 1.25 kHz, regardless of its local variations. It will produce unnecessary samples than required. Moreover, the windowing process is not able to select only the active parts of the sampled signal. In addition, L remains static and is not able to adapt with the signal local variations. Thus, it causes the system to process needless samples and so causes an increased computational activity than the proposed case. For classical case, fixed $N = 4096$ will produce nine fixed $L = 3.3$ second windows, for the total $x(t)$ time span of 30 seconds. It will lead to fix $\Delta t = 3.3$ seconds and $\Delta f = 0.31$Hz for all nine windows (cf. (10) and (11) .

4. COMPUTATIONAL COMPLEXITY

This section compares the computational complexity of the ARSTFT with the classical STFT. The complexity evaluation is made by considering the number of operations executed to perform the algorithm.

In the classical case, Fs is fixed. In this case, a time invariant, fixed L, cosine window function is employed to window the sampled data. If N is the number of samples lie in the window then the windowing operation will perform N multiplications between w_n and x_n (cf. (9)). The spectrum of the windowed data is obtained by computing its DFT. A complex term is involved in the DFT computation. The DFT complexity is calculated by taking the real and the imaginary parts separately. The DFT performs $2\cdot(N)^2$ additions and $2\cdot(N)^2$ multiplications, thus operations count becomes $4\cdot(N)^2$ for N output frequencies. The combined computational complexity C_1 of the STFT is given by (15). Where, A is the total number of windows occurs for the observation length of $x(t)$.

Table 3: Summary of the computational gain.

Time (seconds)	1st activity	2nd activity	3rd activity
Gain = C_1/C_2	2.77	43.43	12.46

For the proposed ARSTFT, Fs^i, Frs^i, and w_n^i are not fixed and are adapted according to the local variations of $x(t)$. The EASA performs $2\cdot N^i$ comparisons and N^i increments for the ith selected window (cf. (Section 2)). The choice of Frs^i and window shape requires three comparisons. The selected signal is resampled before computing its DFT. The NNRI is employed for the resampling purpose. The NNRI only requires a comparison operation for each resampled observation. Therefore, the resampler performs Nr^i comparisons. If $D^i = 0$, then a cosine window function is applied on the resampled data, which performs Nr^i multiplications (cf. (Figure 1)). The DFT performs $4\cdot(Nr^i)^2$ operations for the ith selected window. The combine computational complexity C_2 of the ARSTFT is given by (16). Where $i = 1, 2, \ldots, K$ represents the index of the selected window. α is a multiplying factor, its value is 1 for $D^i = 0$ and 0 for $D^i = 1$. The computational gain of the ARSTFT over the classical one is calculated by employing the results of the illustrative example. The results are summarized in Table 3.

$$C_1 = A\cdot\{N + 4\cdot(N)^2\}. \tag{15}$$

$$C_2 = K\cdot 3 + \sum_{i=1}^{K} 3\cdot N^i + \alpha\cdot Nr^i + Nr^i + 4\cdot(Nr^i)^2. \tag{16}$$

Table 3 shows the computational gain of the ARSTFT over the STFT for each $x(t)$ activity. It shows that the ARSTFT leads to a significant reduction of the total number of operations as compared to the classical one. This reduction in operations is achieved by adapting Fs^i, Frs^i, and w_n^i according to the local variations of $x(t)$.

5. CONCLUSIONS

A new tool for the adaptive resolution time-frequency analysis is proposed. The ARSTFT is especially well suited for the low activity sporadic signals like electrocardiogram, phonocardiogram, seismic signals, and so forth. It is shown that Fs^i and L^i adapt by following the $x(t)$ local variations. Criteria to choose the appropriate F_{ref} and N_{ref} are developed. A complete methodology of adapting Frs^i and w_n^i for the ith selected window has been demonstrated.

The ARSTFT outperforms the STFT. The advantages of the ARSTFT over the STFT are the adaptive time-frequency resolution and the computational gain. These smart features of the ARSTFT are achieved due to the joint benefits of the AADC, the EASA, and the resampling as they enable to adapt Fs^i, Frs^i, N^i, Nr^i, and w_n^i by exploiting the local variations of $x(t)$. The employment of fast algorithms in place of the DFT for the spectrum computation is in progress, it will further add up to the computational efficiency of the ARSTFT. Moreover, the performance comparison of the ARSTFT with other MRA techniques, in terms of computational complexity and quality, opens the way to new research prospective.

REFERENCES

[1] S. C. Sekhar and T. V. Sreenivas, "Adaptive window zero-crossing-based instantaneous frequency estimation," *EURASIP Journal on Applied Signal Processing*, vol. 2004, no. 12, pp. 1791–1806, 2004.

[2] D. Gabor, "Theory of communication," *Journal of the IEE*, vol. 93, no. 3, pp. 429–457, 1946.

[3] R. Polikar, "The engineer's ultimate guide to wavelet analysis," Rowan University, College of Engineering, retrieved in 2006.

[4] M. Vetterli and C. Herley, "Wavelets and filter banks: theory and design," *IEEE Transactions on Signal Processing*, vol. 40, no. 9, pp. 2207–2232, 1992.

[5] H. K. Kwok and D. L. Jones, "Improved instantaneous frequency estimation using an adaptive short-time Fourier," *IEEE Transactions on Signal Processing*, vol. 48, no. 10, pp. 2964–2972, 2000.

[6] J. Mark and T. Todd, "A nonuniform sampling approach to data compression," *IEEE Transactions on Communications*, vol. 29, no. 1, pp. 24–32, 1981.

[7] S. M. Qaisar, L. Fesquet, and M. Renaudin, "Computationally efficient adaptive rate sampling and filtering," in *Proceedings of the 15th European Signal Processing Conference (EUSIPCO '07)*, pp. 2139–2143, Poznan, Poland, September 2007.

[8] M. Gretains, "Time-frequency representation based chirp like signal analysis using multiple level crossings," in *Proceedings of the 15th European Signal Processing Conference (EUSIPCO '07)*, pp. 2154–2158, Poznan, Poland, September 2007.

[9] K. M. Guan and A. C. Singer, "Opportunistic sampling by level-crossing," in *Proceedings of the IEEE International Conference on Acoustics, Speech and Signal Processing (ICASSP '07)*, vol. 3, pp. 1513–1516, Honolulu, Hawaii, USA, April 2007.

[10] E. Allier, G. Sicard, L. Fesquet, and M. Renaudin, "A new class of asynchronous A/D converters based on time quantization," in *Proceedings of the 9th IEEE International Symposium on Asynchronous Circuits and Systems (ASYNC '03)*, pp. 196–205, Vancouver, BC, Canada, May 2003.

[11] N. Sayiner, H. V. Sorensen, and T. R. Viswanathan, "A level-crossing sampling scheme for A/D conversion," *IEEE Transactions on Circuits and Systems II*, vol. 43, no. 4, pp. 335–339, 1996.

[12] F. Akopyan, R. Manohar, and A. B. Apsel, "A level-crossing flash asynchronous analog-to-digital converter," in *Proceedings of the 12th IEEE International Symposium on Asynchronous Circuits and Systems (ASYNC '06)*, pp. 12–22, Grenoble, France, March 2006.

[13] S. M. Qaisar, L. Fesquet, and M. Renaudin, "Spectral analysis of a signal driven sampling scheme," in *Proceedings of the 14th European Signal Processing Conference (EUSIPCO '06)*, Florence, Italy, September 2006.

[14] F. Aeschlimann, E. Allier, L. Fesquet, and M. Renaudin, "Asynchronous FIR filters: towards a new digital processing chain," in *Proceedings of the 10th IEEE International Symposium on Asynchronous Circuits and Systems (ASYNC '04)*, pp. 198–206, Crete, Greece, April 2004.

[15] S. de Waele and P. M. T. Broersen, "A time domain error measure for resampled irregular data," in *Proceedings of the 16th IEEE Instrumentation and Measurement Technology Conference (IMTC '99)*, vol. 2, pp. 1172–1177, Venice, Italy, May 1999.